DEUTSCHES ELEKTRONEN–SYNCHROTRON DESY
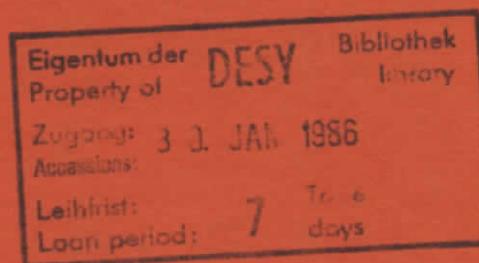
CONTRAST INVESTIGATIONS OF SURFACE ACOUSTIC WAVES

BY STROBOSCOPIC TOPOGRAPHY

III. Contrast in Transmission Case

by

H. Cerva

Inst. f. Angew. u. Techn. Physik, Techn. Universität Wien

W. Graeff

Hamburger Synchrotronstrahlungslabor HASYLAB at DESY

To be sure that your preprints are promptly included in the
HIGH ENERGY PHYSICS INDEX ,
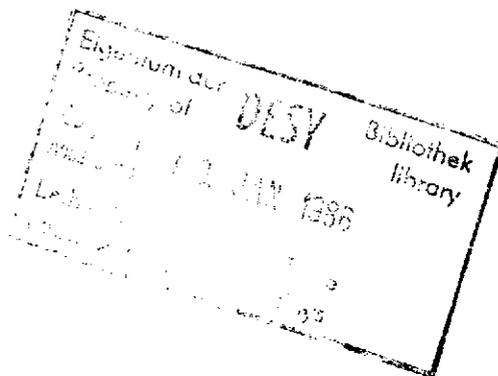send them to the following address (if possible by air mail) :

DESY
Bibliothek
Notkestrasse 85
2 Hamburg 52
Germany

Contrast Investigations of Surface Acoustic Waves
by Stroboscopic Topography

III. Contrast in Transmission Case

By

H. CERVA[1] and W. GRAEFF

Hamburger Synchrotronstrahlungslabor HASYLAB at Deutsches

Elektronen-Synchrotron DESY, Notkestr. 85, D-2000 Hamburg 52, FRG

Introduction

The time structure of synchrotron radiation sources enables stroboscopic X-ray topography. In Bragg case topography, the contrast arising from travelling surface acoustic waves (SAW) on YZ-LiNbO$_3$ crystals was successfully studied in two previous papers by the authors /1,2/. The contrast was traced back to two origins. First, the corrugated crystal surface causes the reflected X-rays to be focussed by wave troughs and defocussed by wave crests, thus forming the dominating orientation contrast. Second, X-rays of the incoming white beam entering the crystal outside the reflection range (in k-space) form wavefield beams which are deviated by the acoustic strain field. Some of these beams can emerge at the entrance surface and give rise to wavefield deviation contrast. These two contrast contributions are always present in the Bragg case and superpose with the contrast of other excited acoustic wave modes.

In this note we report for the first time on the imaging of SAW in the Laue case. The problems arising in contrast investigation in relation to special features of SAW-propagation will be discussed. Transmission topography might prove useful to study bulk waves which are usually coexcited with SAW.

Experimental set-up

The experiments were carried out with synchrotron radiation from the storage ring DORIS. Its parameters and the set-up of the YZ-LiNbO$_3$ crystals were described in /1/. The usual mounting of the SAW device (see Fig. 2 in /1/) was slightly modified in order to permit X-ray transmission. In contrast to the specimens used for reflection topography which were 0.5 mm thick and had a rough bottom surface, the crystals were ground to a thickness of about 300 μm and Syton polished successively. There was one interdigital transducer with a center frequency of 35 MHz corresponding to an acoustic wavelength of Λ = 97.304 μm. The applied signal was 35.4 MHz (a multiple of the single bunch frequency of DORIS) with a peak to peak voltage of 15 V. The acoustic wavelength is then Λ = 98 μm.

[1] Institut f. Angewandte u. Technische Physik, Techn. Univ. Wien, Karlsplatz 13, A-1040 Wien, Austria. Now at: Siemens AG, Forschungslaboratorien, Otto Hahn Ring 6, D-8000 München 83, FRG.

Results and discussion

A SAW travelling on a Y-cut $LiNbO_3$ crystal in Z-direction is completely described by two mechanical displacements u_t (transversal-parallel to Y) and u_l (longitudinal-parallel to Z) and by its quasistatic potential φ. Thus the motion of a volume element is elliptical and in the sagittal-plane of the SAW. This is because lithium niobate is of the trigonal point group symmetry 3m and therefore the sagittal-plane (this is the $2\bar{1}.0$) plane is a mirror plane. In general, however, the elliptical motion involves the third mechanical displacement and is not confined to the sagittal-plane /3/. As can be seen from Fig. 1 the $(2\bar{1}.0)$ plane remains "flat" (i.e. it is not affected by the mechanical elongations) in this case. Lattice defects are usually characterized by their desplacement field $\vec{u}$. In X-ray topography and transmission electron microscopy lattice defect analysis is carried out by finding reflections g where the dot product $\vec{g} \cdot \vec{u}$ gives zero (invisibility criterion). Then the contrat of the defect vanishes (for highly anisotropic crystals, however, there remains a residual contrast) and $\vec{u}$ can be determined /4,5/.

The two topographs in Fig. 2 were taken with the reflections g = (00.3) and $\vec{g}$ = $(2\bar{1}.0)$ (harmonic reflections are present in each case due to the white beam). Since the reflection $\vec{g}_{00.3}$ is parallel to u_l and normal to u_t the contrast of the SAW in Fig. 2a stems from the longitudinal component only. In Fig. 2b the SAW is out of contrast because both u_l and u_t are normal to the reflection $\vec{g}_{2\bar{1}.0}$. Surface waves which are diffracted at the aperture of the interdigital transducer and waves reflected from the rim of the crystal can be seen in both topographs. These SAWs are described by all three mechanical displacements owing to propagation directions off the Z-axis. Moreover, in Fig. 2b (see letter A) a spurious wave travels along the X-axis which was also observed in the reflection topographs /1/. From the transmission topograph the additional information is obtained that this wave has also a displacement component in X-direction. When the acoustic transducer is driven far from its center frequency bulk waves are generated and could be imaged clearly in the $(2\bar{1}.0)$ reflection thus avoiding superposition with SAW contrast.

Contrast simulation of the SAW in the Laue case is much more complicated than in the Bragg case as in the latter coherent superposition of wave fields at the exit point need not to be considered.

In this case, however, the dynamical theory of X-ray diffraction in a slightly deformed crystal /6/ must be extended by the calculation of phase integrals along the trajectory as it was done in a similar case /7/. The simulation of the contrast by the Takagi-Taupin theory /8/ would also need an extension to the algorithm, usually applied, as much of the contrast is due to the wavefront distortion of the exit wave (in /1,2/ refered to as orientation contrast) which results in focussing effects in the vacuum.

With a SAW wavelength of about 100 μm and a substrate thickness of 300 μm the crystal cannot any longer be assumed to be of infinite thickness. The crystal must be regarded as a thin plate with a second polished surface where reflected waves and special plate modes should be taken into account. As a consequence the SAW on the upper boundary has a residual amplitude at the lower boundary which was verified by taking a reflection topograph from the bottom surface. These two surface waves interact with each other and must be considered as a coupled system /3,9/. This, however, has not yet been observed experimentally in stroboscopic topography.

References

/1/ H. CERVA, W. GRAEFF, phys.stat.sol. (a) 82, 35 (1984).

/2/ H. CERVA, W. GRAEFF, phys.stat.sol. (a) 87, 507 (1985).

/3/ A.A. OLINER, (Ed.), Topics in Applied Physics, Vol. 24, Springer-Verlag, 1978, Chap. 1

/4/ B.K. TANNER, X-Ray Diffraction Topography, Pergamon Press, 1976.

/5/ P.B. HIRSCH, A. HOWIE, R.B. NICHOLSON, D.W. PASHLEY, M.J. WHELAN, Electron Microscopy of Thin Crystals, London, Butterworths, 1965.

/6/ U. BONSE, Z.Phys. 177, 385 (1964).

/7/ R. TEWORTE, Acta Cryst. A40, C-354 (1984).

/8/ Y. EPELBOIN, A. SOYER, Acta Cryst. A41, 67-72 (1985).

/9/ B.A. AULD, Acoustic Fields and Waves in Solids, Vol. 2, John Wiley, 1973, Chap. C. 3.

Figure Captions

Figure 1 Sketch illustrating the mechnical displacements u_l and u_t of a SAW propagating in Z-direction on Y-cut $LiNbO_3$. X,Y,Z are rectangular crystal axis. $\vec{K}$ is the acoustic wavevector. Two major crystal planes used for the topographs in Fig. 2 are indicated.

Figure 2 (a) Transmission topograph of SAW propagating on YZ-$LiNbO_3$. Letter A marks the area of the interdigital transducer. Crystal thickness approximately 300 µm. Parameters: 33 mA, 1 s exposure time, $\Theta = 10°$, (00.1), $1 = 3,6$ reflections. $\vec{h}$ indicates the projection of the diffraction vector onto the film, filmdistance 11 cm.
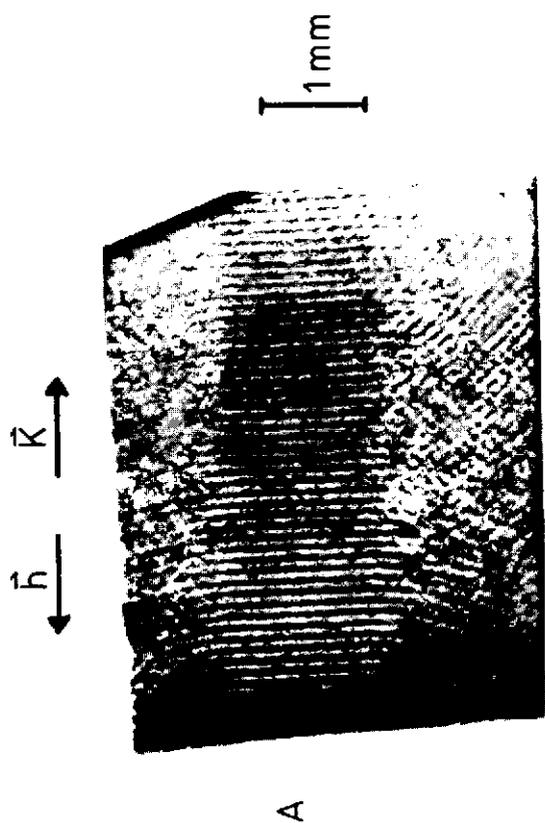(b) SAW is out of contrast with (2k$\bar{k}$.0), k = 1,2 reflections, $\Theta = 3.8°$. SAW parameters are 35.4 MHz, $\Lambda = 98$ µm, 15 V_{pp}.
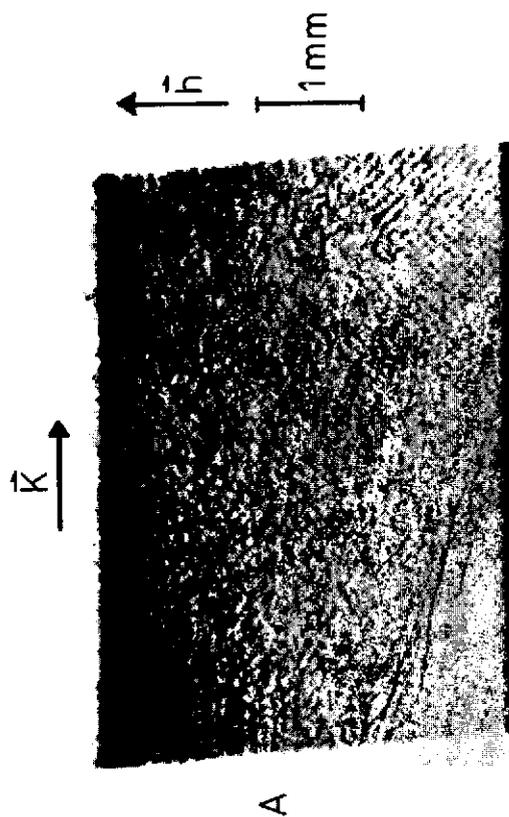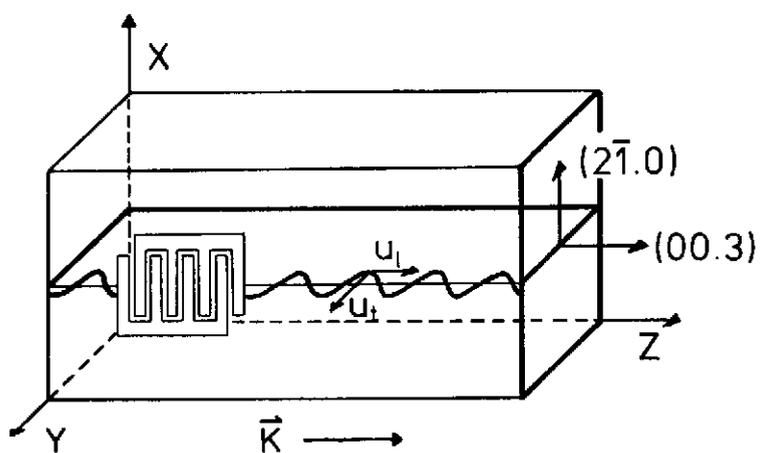
FIGURE 2a

FIGURE 2b

FIGURE 1